UCRL-TR-236131

LAWRENCE
LIVERMORE
NATIONAL
LABORATORY

Fault Geomechanics and Carbon Dioxide Leakage Applied to Geological Storage: FY07 Quarterly and Summary Reports

S. J. Friedmann, J. Morris

November 5, 2007

This work performed under the auspices of the U.S. Department of Energy by Lawrence Livermore National Laboratory under Contract DE-AC52-07NA27344.

FY07 Quarterly and Summary Reports

“Fault Geomechanics and Carbon Dioxide Leakage Applied to Geological Storage”

FWP FEW0149

Lawrence Livermore National Laboratory
Energy and Environmental Directorate
7000 East Avenue
Livermore, California 94550-9234

Contacts:
S. Julio Friedmann
Ph: (925) 423-0585
Email: friedmann@llnl.gov

Joseph Morris
Ph:
Email:

Submitted to:
U.S. Department of Energy
National Energy Technology Manager
DOE Project Manager:
Karen Cohen
Ph: (412) 386-6667
Email: cohen@netl.doe.gov

Period ending:
September 30, 2007

Fault Geomechanics and Carbon Dioxide Leakage Applied to Geological Storage

S. Julio Friedmann, Joseph Morris
Lawrence Livermore National Laboratory

Summary
Safe and permanent storage of carbon dioxide in geologic reservoirs is critical to geologic sequestration. The objective of this study is to quantify the conditions under which a general (simulated) fault network and a specific (field case) fault network will fail and leak carbon dioxide out of a reservoir. Faults present a potential fast-path for CO_2 leakage from reservoirs to the surface. They also represent potential induced seismicity hazards. It is important to have improved quantitative understandings of the processes that trigger activity on faults and the risks they present. Fortunately, the conditions under which leakage along faults is induced can be predicted and quantified given the fault geometry, reservoir pressure, an in-situ stress tensor.

We proposed to expand the current capabilities of fault threshold characterization and apply that capability to a site where is CO_2 injection is active or planned. Specifically, we proposed to use a combination of discrete/explicit and continuum/implicit codes to provide constrain the conditions of fault failure. After minor enhancements of LLNL's existing codes (e.g., LDEC), we would create a 3D synthetic model of a common configuration (e.g., a faulted dome). During these steps, we will identify a field site where the necessary information is available and where the operators are willing to share the necessary information. We would then execute an analysis specific to the field case. The primary products by quarter are listed below.

1Q: Identification of likely field case
2Q: Functioning prototype fault model
3Q: Execution of fault-slip/migration calculation for synthetic case
4Q: Begin simulation of fault-slip/migration calculation for field system

It is worth noting that due to the continuing resolution, we did not receive any funds until 3Q, and did not receive >65% of the support until 4Q. That said, we were still able to meet all of our milestones for FY07 on time and on budget.

Auspice Statement:

This work performed under the auspices of the U.S. Department of Energy by Lawrence Livermore National Laboratory under Contract DE-AC52-07NA27344

1Q: Identify likely field case

In order to accurately represent the field case, it was important to have both geometric and stress information from the site. We identified a number of potential sites, including In Salah (Algeria), SECARB's Phase II site at Cranfield (Missisippi), and BP's Carson Project (California). These and other sites were promising. Ultimately, In Salah proved to be the best site due to BP's willingness, abundant high quality data, and faults that were likely to respond to CO2 injection pressure transients (Figure 1). Our initial engagement with In Salah and BP ultimately led to the agreement to extend this work into In Salah for FY08-10 (see below).

Ultimately, the only site we were able to obtain all the data we needed to execute the 4Q deliverable within FY07 was Teapot Dome. Since this site is federally owned, all information from the site was available in the public domain. We were able to obtain this information from Laura Chiaramonte, a Stanford graduate student working on the site.

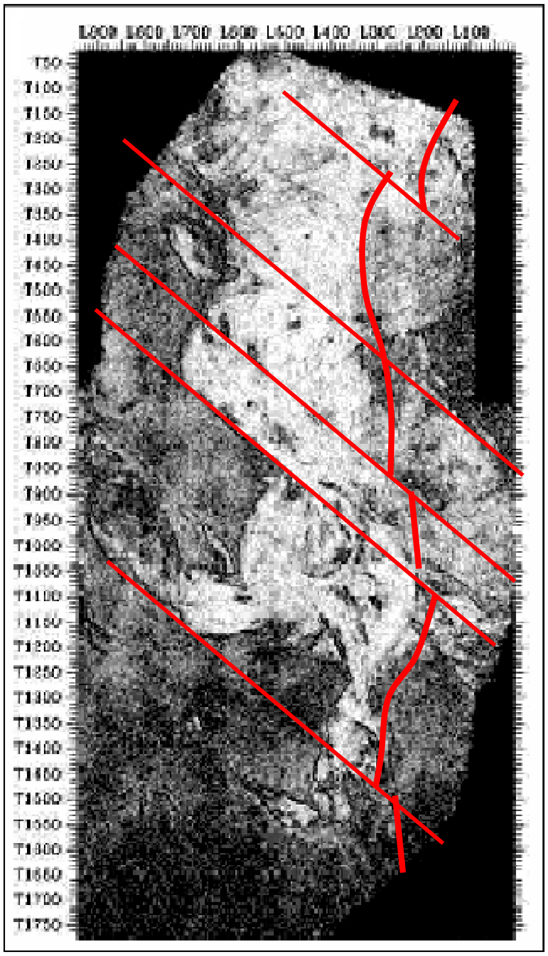

Figure 1: Seismic coherence slice through the Kretchba gas field primary reservoir, central Algeria. The red lines are interpreted faults. The white regions are areas of elevated porosity (sandstones) that hold gas or water, vs. the darker areas (shales)

2Q: Update existing codes for geomechanics; model prototype

LLNL had developed internally a number of codes for geomechanics work. These included GEODYN, which is a continuum code, and two discrete codes: LDEC and FRAC-HMC.

- LLNL's proprietary LDEC code (Morris et al., 2003; Johnson et al., 2005) calculates fluid-pressure driven deformations of the fractured rock mass at different scales. LDEC can be used to simulate normal and/or shear deformation along individual fractures or faults as well as networks of fractures with arbitrary orientation, length, and mechanical properties. All of the elements (rock blocks) can deform independently potentially resulting in slip and/or dilation of existing fractures due to changing pore pressures.
- FracHMC is a recently developed discrete-fracture-network flow code that accommodates stress-induced changes in transmissivity (Detwiler et al., 2006)

During this phase, work began to couple these two codes together. This will provide estimates of changes in effective permeability caused by altered transmissivities of individual fractures within the fracture networks, and will be continued in the next phase.

In addition, the equations of state for CO_2 were added to both codes during 2QFY07, so that they could represent CO_2-fluid mechanical responses accurately (Figure 2). Pore pressure evolution due to fluid injection was added to LDEC to predict resulting fault slippage. Also, post-failure redistribution of stress is included in the analysis in order to provide an understanding of fault network effects and post-failure events.

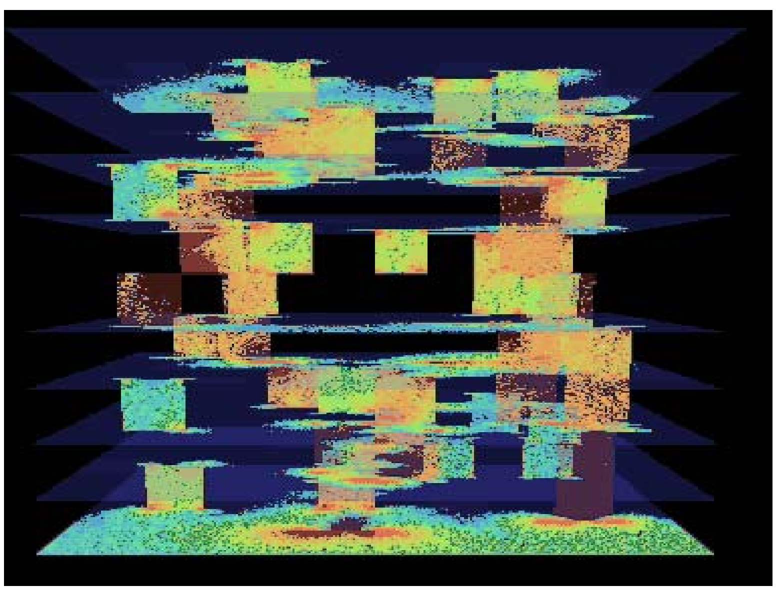

Figure 2: CO_2 migration and dissolution through a complex fracture network in Frac-HMC. The colors represent the change in fracture aperture due to pressure and chemical gradients.

3Q: Model of a synthetic case

The updates and changes in LDEC and Frac-HMC made it possible to begin to analyze in detail simulated cases of fault slip. Two cases were run. The first case had a steeply dipping fault, and the second had a shallowly dipping fault (Figure 3). Both faults were within isotropic, hydrostatic stress fields. CO_2 was injected at a point close to the fault surface within a reservoir, and the pressure increased within the system from continuous injection. The pressure increased stress until the fault failed.

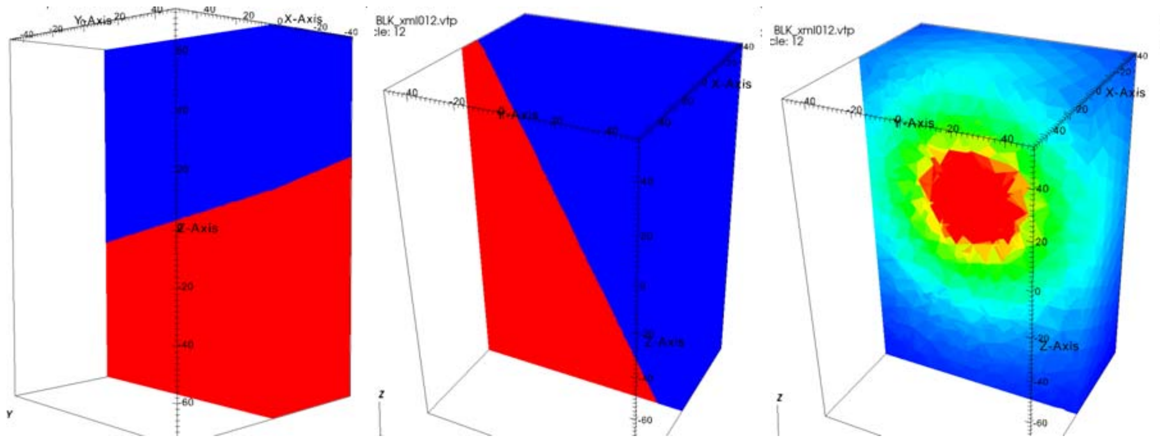

Figure 3: Synthetic fault geometries and stress fields. (LEFT) Shallow (20º) fault model. (Center) Steep (70º) fault model. (Right) Pressure field associated with CO2 injection in reservoir unit at intersection point with the steep fault plane. The discrete structural elements are clearly visible.

A number of features and learnings resulted from the simulated injection tests (Figure 4):

- The high-angle fault failed at a lower deviatoric stress than the low-angle fault
- Both failure events were followed by stick-slip behavior as stress redistributes along the fault plane and within the rock volume
- Failure recurs at the same threshold or envelope (here the ratio of normal and sheer stress of ~0.58, which is an simulation boundary condition)

These results show features and behaviors consistent both with observed behavior on critically stressed faults, suggesting that the tools can accurately represent the key subsurface geomechanical properties. The precision of the models is discussed in the next section.

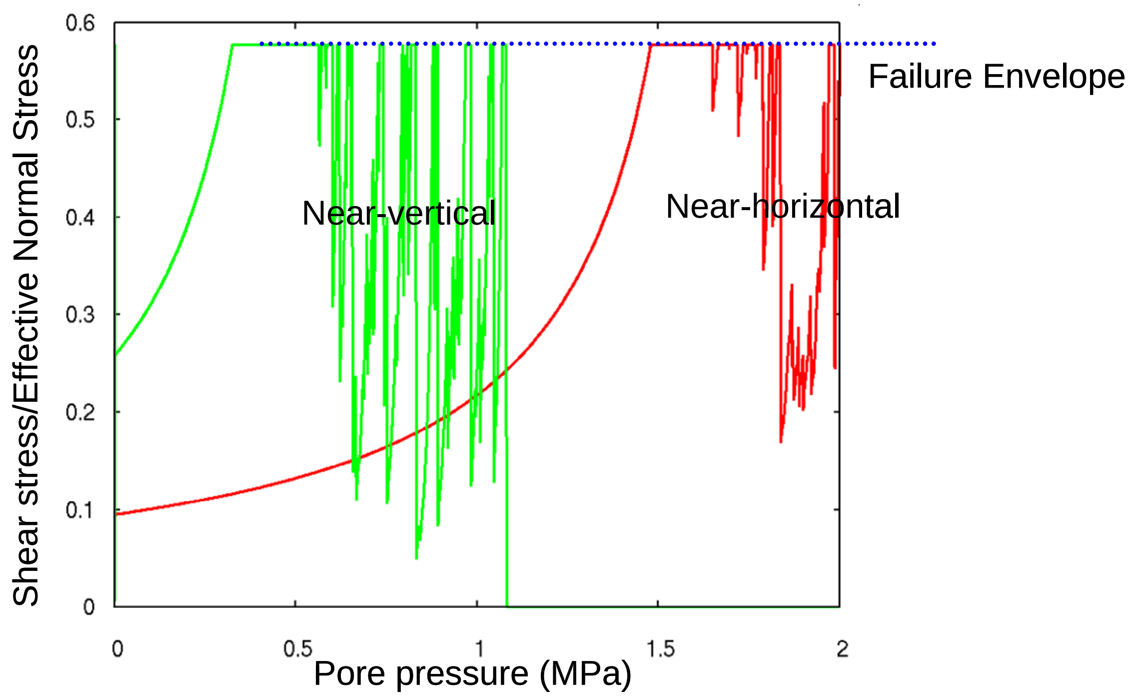

Figure 4: Synthetic fault geometries and stress fields. The near-vertical fault is green, and the near-horizontal fault is in red. Note the lower failure threshold for the near-vertical fault system. The oscillatory failure events is typical of stick-slip behavior in fault systems, as is the exponential growth in shear/normal stress ratio with increased pressure.

4Q: Preliminary Study of Fault Activation at Field Site

The final deliverable was to apply these tools to a specific site of interest. Teapot Dome was selected due to a combination of availability of site data and prior work.

The first phase of our study of Teapot Dome was to acquire data employed by a previous study (Chiaramonte et al., 2007). Once the data was acquired, we attempted to reproduce the results obtained by Chiaramonte et al. (2007) using our own in house implementation of the tools they employed. Using this approach, we considered the projection of the measured in situ stress field onto detailed discretization of the S1 fault and calculated the pore pressure increase that would result in slip at any location of the fault (see Figure 5). The results we obtained differed slightly from Chiaramonte et al. (2007) and further investigation by Chiaramonte (private communication) revealed an error in their analysis which brought our collective results into agreement. The revised results will be the subject of a note to *Environmental Geology*. In other words, *the precision of the LLNL models was high enough to find algebraic errors in prior work around the same system.*

The second phase of our study of Teapot Dome was to apply LLNL specific tools (LDEC) to study the potential for fault activation during injection. Using this approach, we built finite element models of the rock masses surrounding the S1 fault and explicitly simulated the compression and shear on the fault interface. A CO_2 point source was introduced and we simulated fault activation as a function of injection rate. To put this in context, the analysis of Chiaramonte et al. (2007) analyzed the fault surface at discrete locations and identified the level of elevated pore pressure required to activate a given location on the fault in isolation. In contrast, this work presents an approach where the interactions of all locations on the fault are considered in response to specific injection scenarios (for example, with LDEC, as regions of the fault fail, the shear load is taken up elsewhere on the fault).

We developed a process for importing the specific fault geometry used by Chiaramonte et al. (2007) into the LDEC model. However, geometry files suitable for this treatment were delivered too late to be included in the analysis presented here. This report considers a simulation with a single planar fault (see Figure 6) with similar boundary conditions (1200 -2400m domain depth; alignment of the x-axis with the Sig_Hmax direction in the field, y-axis with the Sig_Hmin direction, and z-axis is vertical.

The results of this study are consistent with Chiaramonte et al. (2007). Specifically, given the assumed in situ stress state on the fault (Sig_Hmax ~ Sig_V, with Sig_Hmax acting almost normal to the fault) significantly elevated pore pressure is required to activate the S1 fault. The specific case considered corresponds to point injection at a depth of 1800m, approximately 160m laterally away from the fault. Figure 7 shows the area of fault activated in the simulation as a function of elevation in pore pressure at the location on the fault closest to the injection point. The fault starts to activate when the pore pressure is elevated by approximately 30MPa (~4350 psi) at the location on the fault closest to the injection point. This is well above the deviatoric stress found in operations of this kind.

The fault area activated rapidly grows with increasing pore pressure as load is transferred to neighboring locations on the fault.

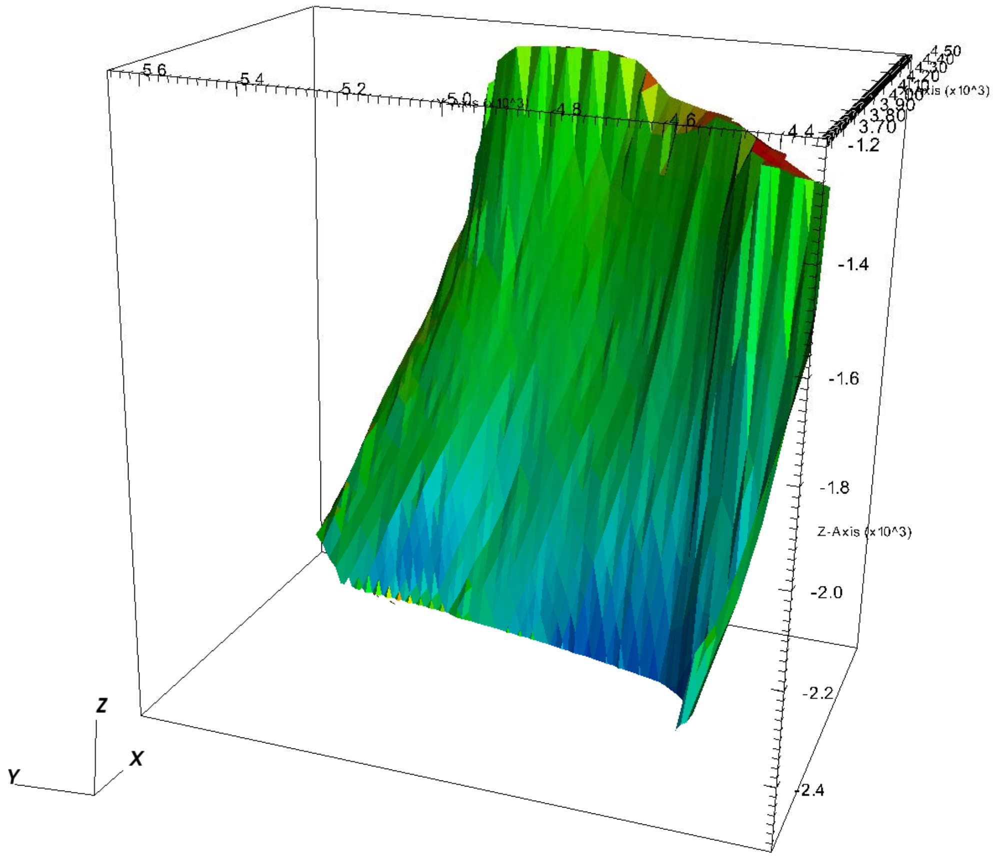

Figure 5: Prediction of pore pressure increase required to activate the S1-fault using in house LLNL implementation of the methodology of Chiaramonte et al. (2007). Blue corresponds to an increase of 35 MPa pore pressure to activate the fault.

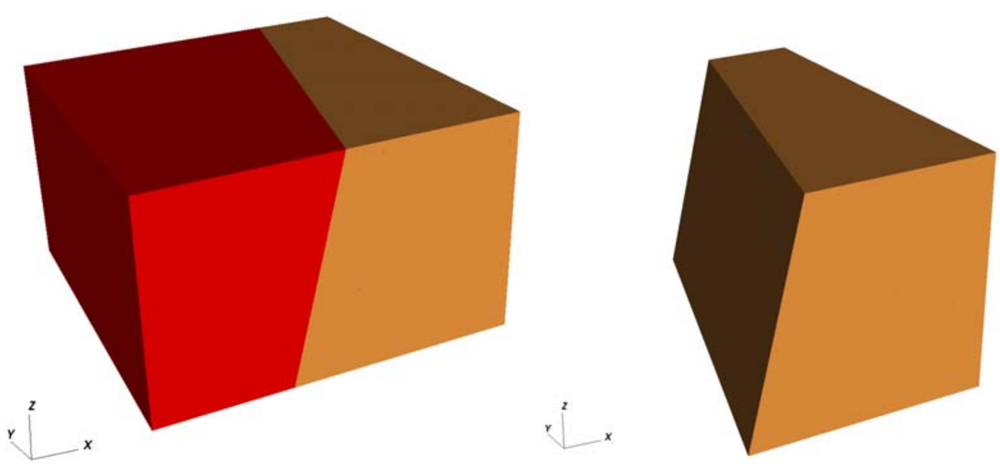

Figure 6: Simplicied LDEC geometry of the S1 fault region. The domain spanned a depth of 1200m through 2400m. The coordinate system has the x-axis aligned with the Sig_Hmax direction, y-axis is aligned with the Sig_Hmin direction and z-axis is vertical.

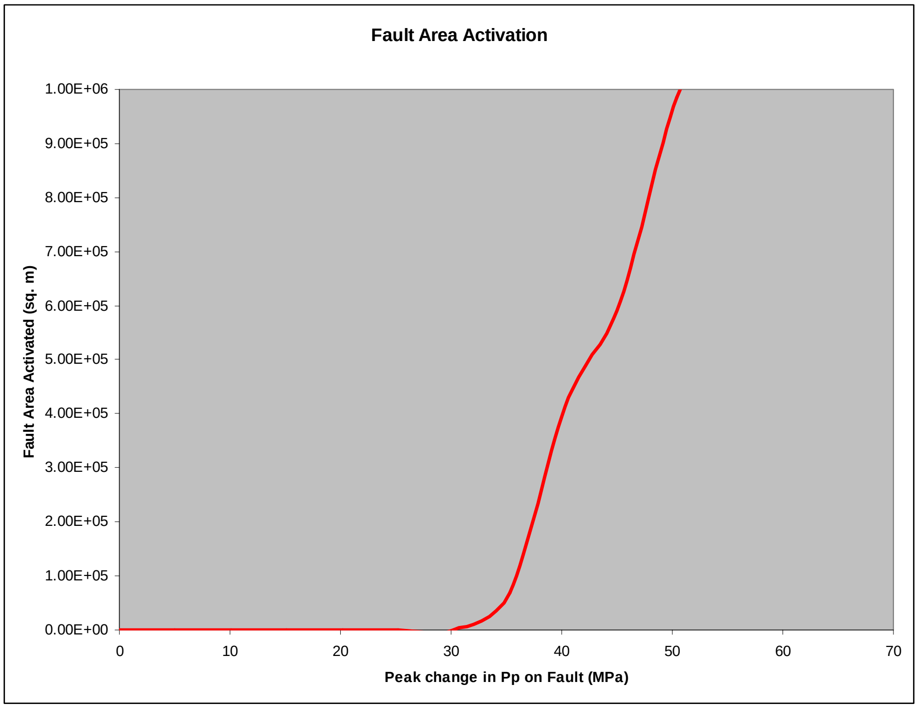

Figure 7: Plot of area of fault that has slipped as a function of the elevation in pore pressure at the location on the fault closest to the injection point (a depth of ~1800m). The fault starts to activate when the pore pressure is elevated by approximately 30MPa at this location. The fault area activated rapidly grows with increasing pore pressure as load is transferred to neighboring locations on the fault.

FY08 Plan

These results can be readily applied to the continuation of this work in FY08. In particular, we expect that the injection and pressure data from In Salah, the new overburden model, and the complex fault geology can all be handled properly given the experience with these codes and the ability to move files into the necessary software.

References

Chiaramonte, L., M. D. Zoback, J. Friedman, V. Stamp, “Seal integrity and feasibility of CO2 sequestration in the Teapot Dome EOR pilot: geomechanical site characterization,” *Environ. Geol.*, 2007.

Detwiler, R.L., J.P. Morris and S.M. Ezzedine, Coupling micromechanics and fluid flow through discrete fracture networks: Quantifying effective permeability under variable stress conditions, *Eos Transactions AGU*, 86(46), Fall Meeting Supplement, Abstract H13D-1433, 2006.

Johnson, J.W., Nitao, J.J., and Morris, J.P., 2005, Reactive transport modeling of cap rock integrity during natural and engineered CO_2 storage: in *Carbon Dioxide Capture for Storage in Deep Geologic Formations: Vol. 2*, Thomas, D.C., and Benson, S.M., eds., p. 787-813.

Morris, J.P., M. B. Rubin, S. C. Blair, L. A. Glenn and F. E. Heuze, Simulations of Underground Structures Subjected to Dynamic Loading using the Distinct Element Method, *Engineering Computations,* Vol. 21 (2/3/4), 384-408, 2003.